

Impact of a single high-rise building on the wind pressure acting on the surrounding low-rise buildings

Yuta Yamane¹, Shuhei Kamata², Yasuyuki Ishida³, Akihito Yoshida⁴, Akashi Mochida⁵

¹ Graduate School of Eng., Tohoku University, Sendai, Japan, yamane.yuta.r4@dc.tohoku.ac.jp

² Graduate School of Eng., Tohoku University, Sendai, Japan, shuhei.kamata.t5@dc.tohoku.ac.jp

³ Graduate School of Eng., Tohoku University, Sendai, Japan, yasuyuki.ishida.e1@tohoku.ac.jp

⁴ Graduate School of Eng., Tokyo Polytechnic University, Atsugi, Japan,
yoshida@arch.t-kougei.ac.jp

⁵ Graduate School of Eng., Tohoku University, Sendai, Japan, akashi.mochida.d1@tohoku.ac.jp

SUMMARY:

High-rise buildings generate high-wind areas around them. However, the interference effect of high-rise buildings on the surrounding low-rise buildings has not yet been evaluated. In this study, wind tunnel experiments were conducted to investigate the wind pressure coefficient on the roofs and walls of low-rise buildings surrounding a single high-rise building. Overall, 72 different wind directions, ranging from 0° to 355° in 5° increments, were considered, and the effects of wind direction on the wind pressure coefficients of the surrounding buildings were evaluated. For low-rise buildings located downwind of the high-rise building, negative and positive peak wind pressure coefficients occurred when the wind directions were 25°, and 30°, respectively. The negative peak value, which was observed at the upwind end of the roof of the low-rise building, was approximately thrice that of the case without a high-rise building. The fluctuating pressure coefficient in the region of very large negative peak wind pressure exceeded 1.0 [-], which was higher than that in other conditions.

Keywords: high-rise building, wind pressure coefficient, wind tunnel experiment

1. INTRODUCTION

Wind load has been an important issue in the structural design of high-rise buildings, and wind tunnel experiments (Kwok et al., 1988; Tanaka et al., 2012) have been used to quantitatively evaluate the wind pressure acting on building walls. It is well known that high-rise buildings generate strong winds in the surrounding pedestrian space, and studies on the characteristics of strong winds generated by high-rise buildings have been conducted for many years (Murakami et al., 1979; Xu et al., 2017). Furthermore, studies have been conducted on the interference effect of high-rise buildings on the aerodynamic response of buildings to be designed (Khanduri et al., 1998; Kim et al., 2011; Chen et al., 2018). However, there are few studies on how high-rise buildings affect the wind pressure of surrounding low-rise buildings.

In this study, the impact of a single high-rise building on the wind pressure acting on the surrounding low-rise buildings was investigated through wind tunnel experiments on a low-rise urban block with a gross coverage ratio of 25%.

2. EXPERIMENTAL CONDITIONS

The wind tunnel experiments were conducted in a Boundary Layer Wind Tunnel at the Tokyo Polytechnic University. The test section of the wind tunnel was 2.2 m wide, 1.8 m high, and 19 m long. The test model for wind pressure measurement was a 1/200 scale 150 mm cube with 356 measurement taps (Figure 1) and placed at the center of the turntable (Figure 2). Experiments were conducted for six cases (Table 1): five cases with different locations of a high-rise building (750 mm high) and one case with uniform heights (no high-rise). Figure 3 shows a photograph of the model layout of Case 2. Figure 4 shows the characteristics of the approach flow. The velocity scale was set to 1/6 and the time scale was 3/100. Overall, 72 wind directions were considered with 5° increments from 0° to 355°. The sampling frequency was 800 Hz, and 10 samples were acquired for a sampling time of 20 s (10 min on a full time scale). The tube effects were numerically corrected using the gain and phase characteristics of the pressure measurement system.

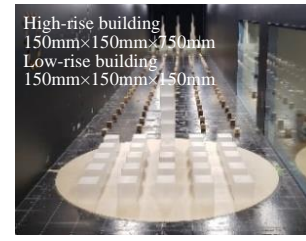
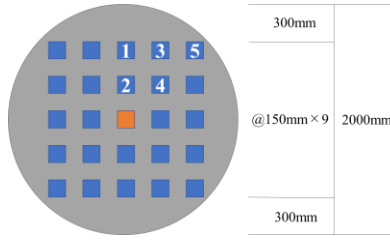
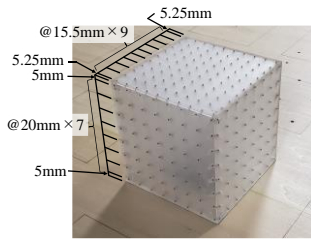


Figure 1. Test model for wind pressure measurement.

Figure 2. Model placement on the turntable.

Figure 3. Photograph of the model layout (Case 2).

Table 1. Experimental cases.

Case Name	Location of a high-rise building (The number in Figure 2)
Case 0	Uniform height (No high-rise building)
Case 1	1
Case 2	2
Case 3	3
Case 4	4
Case 5	5

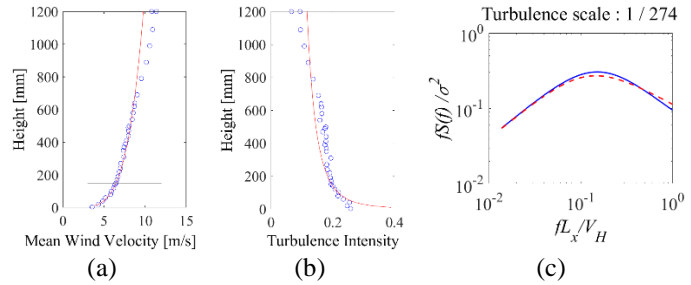


Figure 4. Characteristics of approach flow; (a) mean wind velocity; (b) turbulent intensity; (c) power spectrum density.

The reference velocity pressure $\overline{q_h}$ was obtained from the average wind speed at the roof height of the test model for wind pressure measurement. $\overline{q_h}$ is used to obtain the instantaneous wind pressure coefficient. Moving average of 0.2 s on the full-time scale was applied to the instantaneous pressure to obtain various wind pressure coefficients for 600s on a full time scale. The formulas for calculating the wind pressure coefficient are given in Eqs. (1)-(4). C_p is the wind pressure coefficient for each tap (Eq. (1)), whereas p_i [N/m²] is the wind pressure at each tap. $\overline{C_p}$ [-] is the mean wind pressure coefficient (Eq. (2)). $peakC_p(n)$ [-] is the maximum or minimum wind pressure coefficient at each tap for each sample (Eq. (3)), where n [-] denotes the number of samples. C_p' [-] denotes the fluctuating pressure coefficient at each tap (Eq. (4)), and σ_p [N/m²] is the standard deviation of the wind pressure value at each tap.

$$C_p = \frac{p_i}{\overline{q_h}} \quad (1) \quad \overline{C_p} = \frac{1}{n} \sum_{i=1}^n C_p(i) \quad (2) \quad peakC_p = \frac{1}{10} \sum_{n=1}^{10} peakC_p(n) \quad (3) \quad C_p' = \frac{\sigma_p}{\overline{q_h}} \quad (4)$$

3. RESULTS

3.1. Variations of $peakC_p$ for wind directions and location of a high-rise building

Figure 5 shows the results of the maximum and minimum values of the peak wind pressure coefficient at each pressure measurement point for all wind directions for all the pressure taps. Considering the positive peak wind pressure coefficient, the values are larger around 30° , 65° , 300° , and 330° in Case 2, and around 30° and 65° in Case 5, which are approximately 1.5 times larger than those in Case 0. The negative peak wind pressure coefficients in Case 2 have large negative values around wind angles of 25° and 335° , which are approximately three times larger than those in Case 0, i.e., no high-rise buildings.

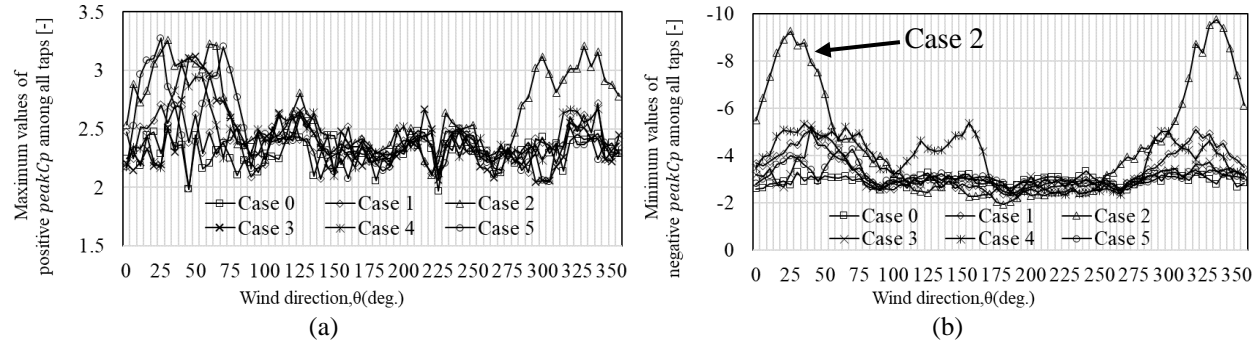


Figure 5. Variations of maximum values of positive $peakC_p$ and minimum values of negative $peakC_p$ among all taps for wind directions and location of a high-rise building; (a) Positive $peakC_p$; (b) Negative $peakC_p$.

3.2. Wind pressure coefficient distribution at 25° wind direction angle (Case 2)

In this section, we analyze the spatial distribution of the wind pressure coefficient for the case with a wind direction angle of 25° , which exhibited the minimum negative peak wind pressure coefficient in Case 2. The results for Case 0, where there were no high-rise buildings, are also shown for comparison. Figure 6 shows the spatial distribution of various wind pressure coefficients when the wind direction is 25° . With respect to the average wind pressure coefficient, a relatively large negative pressure was generated at the upwind corner of the roof surface in Case 2, and a value of approximately four times higher than that in Case 0 can be observed at some pressure taps. For the positive peak wind pressure coefficient, the value was large on the upwind side, and the maximum value in Case 2 was approximately 1.5 times larger than that in Case 0. With respect to the negative peak wind pressure coefficient, a very large negative pressure of approximately -9.3[-], which was approximately three times larger than that in Case 0, was observed at the roof surface corner in Case 2. For the fluctuating wind pressure coefficient, a value exceeding 1.0 was observed at the upwind corner of the roof surface in Case 2, where a large negative peak wind pressure coefficient was observed, indicating that the value is very large compared to that in Case 0. These results suggest that the downwash flow from the high-rise building impinged on the test model during wind pressure measurement and caused a large negative pressure owing to the strong separation on the roof surface of the low-rise building.

4. CONCLUSIONS

In this study, we analyzed the peak wind pressure coefficients of low-rise buildings located near the high-rise building using wind tunnel experiments. When the wind direction angle was 25° , the peak wind pressure coefficient for the low-rise building directly behind the high-rise building was

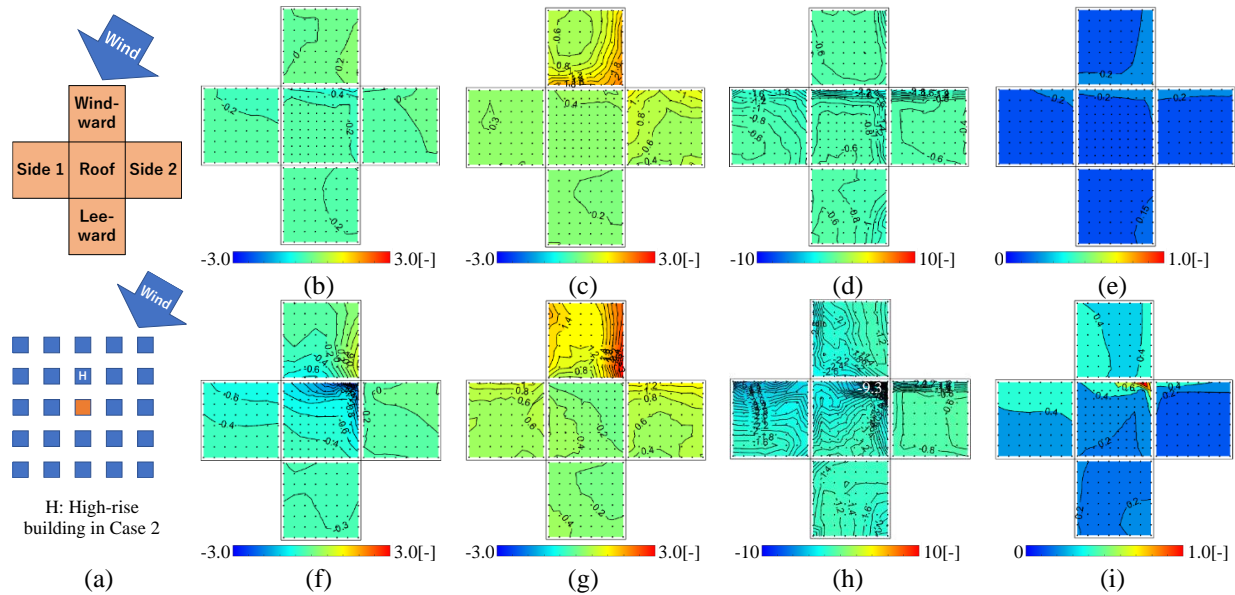


Figure 6. Spatial distribution of various wind pressure coefficients when the wind direction angle is 25° . (a) Building model arrangement and prevailing wind direction in Figures (b) to (j); Top row: Case 0: no high-rise buildings; Bottom row: Case 2 with the high-rise building next to the test model for wind pressure measurement. (b) and (f) represent $\overline{C_p}$; (c) and (g) represent positive *peak* C_p ; (d) and (h) represent negative *peak* C_p ; (e) and (i) represent C_p' .

larger on the positive and negative sides. Particularly, a very large negative peak wind pressure coefficient of approximately $-9.3[-]$, which was approximately three times higher than that without the high-rise building, was generated at the corner of the roof surface. Additionally, the fluctuating pressure coefficient in the region of a very large negative peak wind pressure was greater than $1.0[-]$, indicating that large fluctuations occurred.

ACKNOWLEDGEMENTS

This research was supported by JSPS KAKENHI (Grant Number 21H01486). We would also like to express our gratitude to Takenari Yokoyama, a student at the Tokyo Polytechnic University, for his cooperation in conducting this wind tunnel experiment.

REFERENCES

- Chen, B., Shang, L., Qin, M., Chen, X., Yang, Q., 2018. Wind interference effects of high-rise building on low-rise building with flat roof. *Journal of Wind Engineering and Industrial Aerodynamics* 183, 88–113.
- Kwok, K. C. S., Wilhelm, P. A., and Wilkie, B. G., 1988. Effect of edge configuration on wind-induced response of tall buildings. *Engineering Structure* 10, 135–140.
- Khanduri, A. C., Stathopoulos, T., and Bédard, C., 1998. Wind-induced interference effects on buildings – a review of the state-of-the-art. *Engineering Structure* 20, 617–630.
- Kim, W., Tamura, Y., and Yoshida, A., 2011. Interference effects on local peak pressures between two buildings. *Journal of Wind Engineering and Industrial Aerodynamics* 99, 584–600.
- Murakami, S., Uehara, K., and Komine, H., 1979. Amplification of wind speed at ground level due to construction of high-rise building in urban area. *Journal of Wind Engineering and Industrial Aerodynamics* 4, 343–370.
- Tanaka, H., Tamura, Y., Ohtake, K., Nakai, M., Kim, Y. C., 2012. Experimental investigation of aerodynamic forces and wind pressures acting on tall buildings with various unconventional configurations. *Journal of Wind Engineering and Industrial Aerodynamics* 107-108, 179–191.
- Xu, X., Yang, Q., Yoshida, A., Tamura, Y., 2017. Characteristics of pedestrian-level wind around super-tall buildings with various configurations. *Journal of Wind Engineering and Industrial Aerodynamics* 166, 61–73.